Journal of Biomolecular NMR, 9 (1997) 167–180
ESCOM

J-Bio NMR 417

^{1}H, ^{13}C, and ^{15}N NMR backbone assignments and chemical-shift-derived secondary structure of glutamine-binding protein of *Escherichia coli**

Jinghua Yu, Virgil Simplaceanu, Nico L. Tjandra**, Patricia F. Cottam, Jonathan A. Lukin and Chien Ho***

Department of Biological Sciences, Carnegie Mellon University, 4400 Fifth Avenue, Pittsburgh, PA 15213-2683, U.S.A.

Received 15 August 1996
Accepted 26 November 1996

Keywords: Triple-resonance NMR; Backbone assignment; Glutamine-binding protein

Summary

^{1}H, ^{13}C, and ^{15}N NMR assignments of the backbone atoms and β-carbons have been made for liganded glutamine-binding protein (GlnBP) of *Escherichia coli*, a monomeric protein with 226 amino acid residues and a molecular weight of 24 935 Da. GlnBP is a periplasmic binding protein which plays an essential role in the active transport of L-glutamine through the cytoplasmic membrane. The assignments have been obtained from three-dimensional triple-resonance NMR experiments on a ^{13}C,^{15}N uniformly labeled sample as well as specifically labeled samples. Results from the 3D triple-resonance experiments, HNCO, HN(CO)CA, HN(COCA)HA, HNCA, HN(CA)HA, HN(CA)CO, and CBCA(CO)NH, are the main sources used to make the resonance assignments. Other 3D experiments, such as HNCACB, COCAH, HCACO, HCACON, and HOHAHA-HMQC, have been used to confirm the resonance assignments and to extend connections where resonance peaks are missing in some of the experiments mentioned above. We have assigned more than 95% of the polypeptide backbone resonances of GlnBP. The result of the standard manual assignment is in agreement with that predicted by an automated probabilistic method developed in our laboratory. A solution secondary structure of the GlnBP–Gln complex has been proposed based on chemical shift deviations from random coil values. Eight α-helices and 10 β-strands are derived using the Chemical Shift Index method.

Introduction

Periplasmic transport systems of gram-negative bacteria are responsible for transporting a wide variety of substances, such as sugars, amino acids, peptides, anions, and other nutrients, across the cytoplasmic membrane (Ames, 1986; Furlong, 1987). These transport systems belong to a superfamily of transport systems known as traffic ATPases (Ames and Joshi, 1990) or ATP-binding cassette transporters (Hyde et al., 1990). The bacterial transport systems are composed of a ligand-specific binding protein and a membrane-bound protein complex. The binding proteins are located in the periplasmic space, and act as receptors for a specific ligand. Over 30 periplasmic binding proteins have been characterized. Crystal structures of more than 10 of them have been solved (Ames, 1986; Kang et al., 1991; Spurlino et al., 1991; Vyas et al., 1991; Sharff et al., 1992). Despite wide discrepancies in their primary amino acid sequences, these proteins have similar tertiary structures and interactions with ligands. They all share a two-domain hinged structure in which the cleft between domains provides the ligand-binding site (Quiocho et al., 1987).

Models proposed for periplasmic binding protein-dependent transport consist of several steps (Ames, 1986; Quiocho, 1990). In the recognition step, a given binding protein picks up a specific ligand in the periplasm. Upon ligand binding, the two domains of the binding protein

*Preliminary accounts of the research presented in this paper were given at the 38th and 39th meetings of the Biophysical Society at New Orleans, LA, U.S.A., 1994 and San Francisco, CA, U.S.A., 1995.

**Present address: Laboratory of Chemical Physics, National Institute of Diabetes and Digestive and Kidney Diseases, National Institutes of Health, Bethesda, MD 20892, U.S.A.
***To whom correspondence should be addressed.

undergo a conformational change due to a hinge-bending motion (Newcomer et al., 1981; Mao et al., 1982), which closes the cleft and forms a very compact globular structure. This conformational change appears to be a prerequisite for the recognition of the binding protein–ligand complex by the associated membrane-bound protein components. The interaction between the protein–ligand complex and the membrane-bound proteins activates the energy-coupling mechanism which involves adenosine triphosphate or guanosine triphosphate hydrolysis (Ames and Joshi, 1990; Higgins et al., 1990) and results in the opening of a pore and the subsequent translocation of the ligand across the cytoplasmic membrane. This model provides a general picture of the transport process, but the detailed molecular mechanisms of ligand recognition, binding, and dissociation remain to be understood. A particularly interesting question is why these binding proteins have such a high specificity and affinity for their specific ligands while bearing similar tertiary structures. NMR spectroscopy offers an excellent tool to investigate

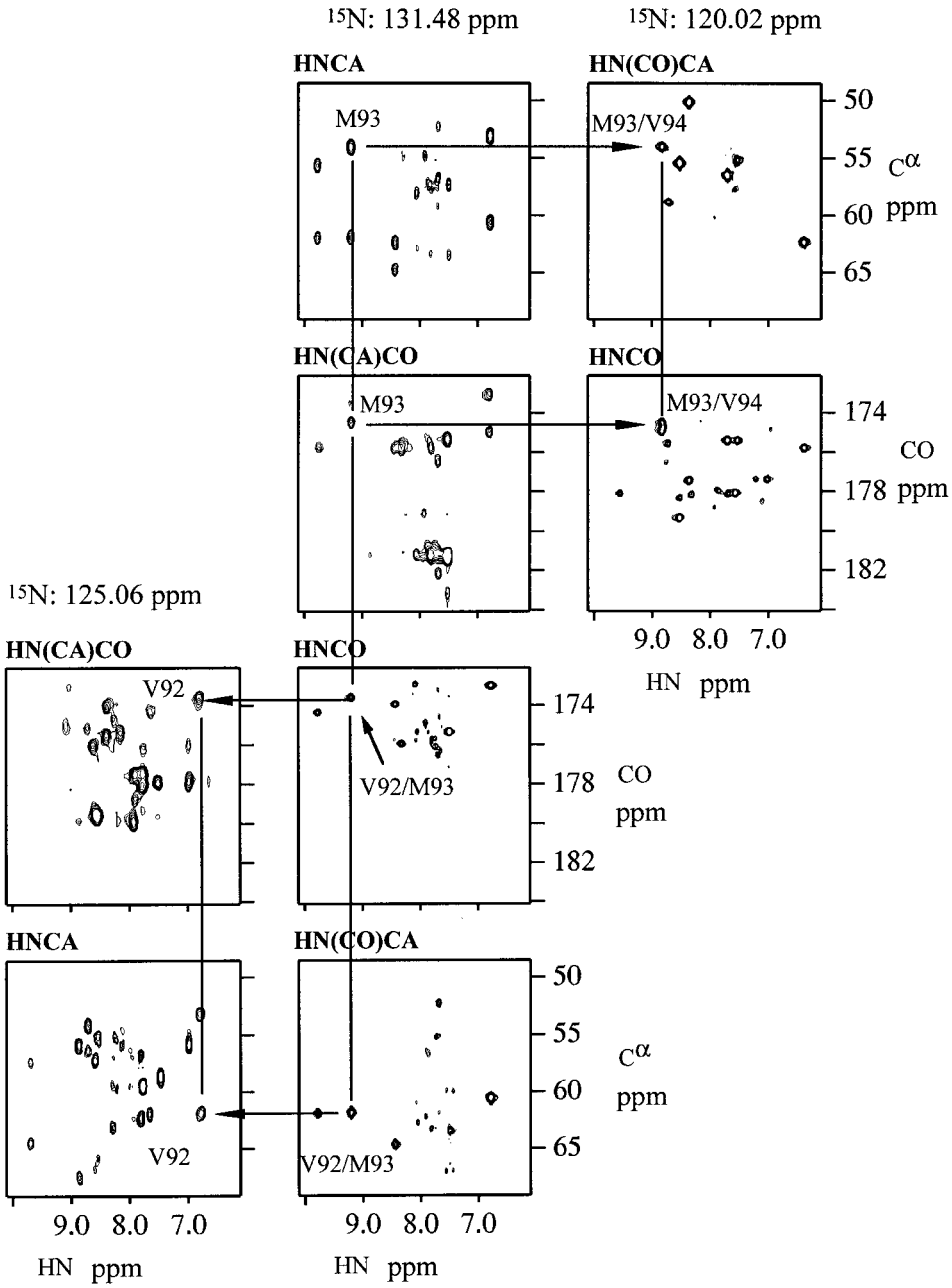

Fig. 1. Polypeptide backbone assignments of Val[92] and Val[94] starting at Met[93], an example to show how to make connections and extend assignments in both directions from a known amino acid residue using the 3D NMR experiments. The HNCA, HN(CA)CO, HNCO, and HN(CO)CA experiments were performed on the ^{13}C,^{15}N uniformly labeled GlnBP–Gln, in 0.1 M phosphate buffer, 10% D_2O, pH 7.2, at 41 °C, using a Bruker AM-500 NMR spectrometer. For details on acquisition, see Table 1.

TABLE 1
ACQUISITION PARAMETERS FOR EXPERIMENTS

Experiment	Nucleus			No. of complex points			Acquisition time (ms)			Scans	Total time (h)
	F1	F2	F3	F1	F2	F3	F1	F2	F3		
HNCO	^{15}N	^{13}CO	$^{1}H^{N}$	27	36	512	16.2	18.8	64	48	64
HNCA	^{15}N	$^{13}C^{\alpha}$	$^{1}H^{N}$	27	32	256	16.2	8.4	32	96	111
HN(CO)CA	^{15}N	$^{13}C^{\alpha}$	$^{1}H^{N}$	28	32	512	16.8	8.4	64	80	98
HN(COCA)HA	^{15}N	$^{1}H^{\alpha}$	$^{1}H^{N}$	26	36	256	15.6	13.7	32	128	156
HN(CA)CO	^{15}N	^{13}CO	$^{1}H^{N}$	27	64	512	16.2	16.7	64	240	240
HN(CA)HA	^{15}N	$^{1}H^{\alpha}$	$^{1}H^{N}$	32	31	512	15.7	7.8	64	112	140
HNCACB	^{15}N	$^{13}C^{\alpha/\beta}$	$^{1}H^{N}$	80	32	512	6.4	14.4	125	16	44
CBCA(CO)NH	$^{13}C^{\alpha/\beta}$	^{15}N	$^{1}H^{N}$	48	25	512	5.9	15.6	128	32	53
HCACO	$^{13}C^{\alpha}$	^{13}CO	$^{1}H^{\alpha}$	32	32	512	7.0	16.7	64	112	127
HCA(CO)N	^{15}N	$^{13}C^{\alpha}$	$^{1}H^{\alpha}$	28	35	512	14.0	6.3	64	96	110
COCAH	$^{13}C^{\alpha}$	^{13}CO	$^{1}H^{\alpha}$	37	17	512	6.6	8.9	64	48	96
HOHAHA-HMQC	^{15}N	^{1}H	$^{1}H^{N}$	24	80	512	14.4	12.8	64	32	84
HSQC	^{15}N	$^{1}H^{N}$		128	512		76.8	64		16	1

these interesting problems associated with the structure–function relationship in periplasmic binding proteins.

The glutamine permease system provides a good model for the NMR study of the essential processes of the periplasmic binding protein-dependent membrane transport. It is a well-characterized bacterial transport system responsible for the active transport of L-glutamine across the cytoplasmic membrane of *Escherichia coli* (Weiner and Heppel, 1971). The binding protein of the system, glutamine-binding protein (GlnBP), is a monomeric basic protein, with 226 amino acid residues and a molecular weight of 24 935 Da. Thus, GlnBP, one of the smallest periplasmic binding proteins, is of a size suitable for study by multidimensional NMR methodologies. It binds L-glutamine with a molar ratio of 1:1 at neutral pH (Weiner and Heppel, 1971; Shen et al., 1989a). The binding process is rapid and reversible (Hunt and Hong, 1983a; Shen et al., 1989a). Two analogues of L-glutamine, γ-glutamylhydrazide and γ-glutamylhydroxamate, also bind to GlnBP (Weiner and Heppel, 1971). The protein is stable within a pH range of 5.0–8.0 and at temperatures up to 41 °C (Weiner and Heppel, 1971; Hunt and Hong, 1981; Tjandra et al., 1992). The crystal structure of unliganded GlnBP has been determined by X-ray diffraction (Hsiao, 1993; Hsiao et al., 1996) and exhibits the two-domain structure typical of periplasmic binding proteins.

In order to understand the high specificity and affinity of GlnBP for its ligand as well as the detailed mechanisms of ligand recognition and binding, a solution structure of the GlnBP–Gln complex is essential. The first step toward a solution structure of a protein is the sequential assignment of the polypeptide backbone resonances (Wüthrich, 1986), which is challenging for GlnBP due to its relatively large size. Experiments performed on specifically labeled GlnBP samples (Tjandra et al., 1992) have provided unambiguous assignments of several amino acid residues which can be used as starting and check points for the complete backbone resonance assignment. Using 2D and 3D heteronuclear NMR techniques developed in recent years, we have achieved the assignment of polypeptide backbone resonances for more than 95% of the amino acid residues. In this paper, we present the ^{1}H, ^{13}C, and ^{15}N NMR assignments of the polypeptide backbone atoms and the β-carbons of GlnBP. In addition, we present the solution secondary structure of the GlnBP–glutamine complex derived from using the chemical shift index (CSI) method (Wishart et al., 1992). This secondary structure is compared to the crystal structure of unliganded GlnBP (Hsiao, 1993; Hsiao et al., 1996).

Materials and Methods

Preparation of GlnBP samples

^{15}N uniformly labeled GlnBP and ^{15}N,^{13}C uniformly labeled GlnBP were prepared from *E. coli* K12 (ATCC #10798). For specific labeling of certain amino acids with ^{15}N or ^{13}C, auxotrophs W3110 *Trp* A33 (a gift from Dr. C. Yanofsky, Stanford University, Stanford, CA, U.S.A.) (Drapeau et al., 1968), KA197 *Phe* A97 and AT2471 *Tyr* A4 (kindly provided by Dr. Barbara Bachmann, *E. coli* Genetic Stock Center, New Haven, CT, U.S.A.), and CM1021 *Pro*, *Met* (constructed in our laboratory) were used. Each strain was transformed with pGP1-2 and pJW133 (gifts of Dr. J.-S. Hong, Boston Biomedical Research Institute, Boston, MA, U.S.A.). Bacteria were grown as described by Tjandra et al. (1992) with minor modifications to accommodate the different auxotrophic requirements. $(^{15}NH_4)_2SO_4$ was used as the ^{15}N source for ^{15}N uniformly labeled GlnBP. D-Glucose-$^{13}C_6$ was used in the minimal medium at a concentration of 2 g/l to produce ^{13}C uniformly labeled GlnBP.

The following specifically labeled samples, obtained from the corresponding auxotrophs, were used in our experiments: [^{15}N-Trp] in which the tryptophan residues

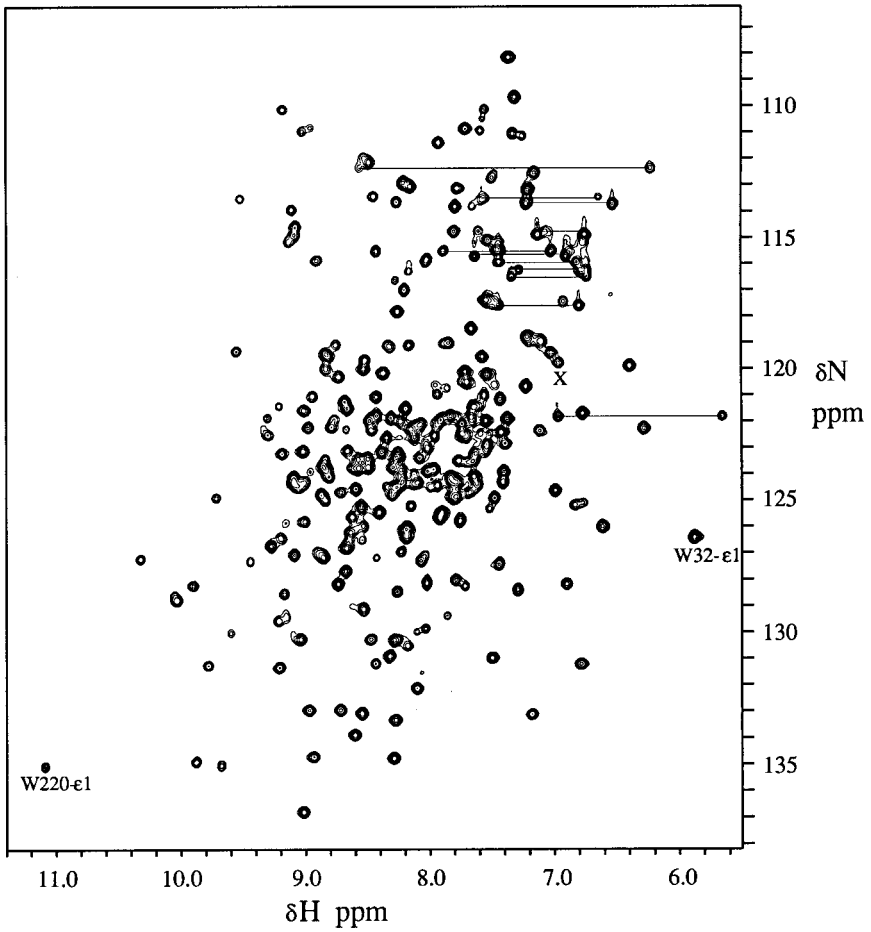

Fig. 2. HSQC spectrum of ^{15}N uniformly labeled GlnBP–Gln in 0.1 M phosphate buffer, 10% D_2O, pH 7.2, at 41 °C, using a Bruker AM-500 NMR spectrometer. The original data size is 512 (F2) × 128 (F1), and the final size is 4096 (F2) × 1024 (F1) with zero-filling in both dimensions and linear prediction in F1. Side-chain NH_2 resonances are linked by lines. The peak labeled X is folded in from a ^{15}N chemical shift of 86.9 ppm.

were labeled with ^{15}N; [$^{13}C'$-Pro,^{15}N-Met] in which methionine residues were labeled with ^{15}N, while the carbonyls of proline residues were labeled with ^{13}C; [$^{13}C'$-Phe,^{15}N-other] and [$^{13}C'$-Tyr,^{15}N-other] in which the carbonyls of phenylalanine or tyrosine residues were labeled with ^{13}C, while other residues were labeled with ^{15}N. All of these samples were prepared in our laboratory.

L-Proline-1-^{13}C, L-tyrosine-1-^{13}C, and L-methionine-^{15}N were purchased from Cambridge Isotope Laboratories (Andover, MA, U.S.A.). D-Glucose-$^{13}C_6$, L-phenylalanine-1-^{13}C, and $(^{15}NH_4)_2SO_4$ were purchased from Isotec Inc. (Miamisburg, OH, U.S.A.), and L-tryptophan-^{15}N was purchased from Merck.

GlnBP was purified according to our published procedure (Shen et al., 1989a). Protein samples were dissolved in 100 mM phosphate buffer, pH 7.2, with 0.02% NaN_3. Excess L-glutamine (two–threefold) was added to each sample to make sure that GlnBP was in the liganded form. One ^{15}N,^{13}C uniformly doubly labeled GlnBP sample was in D_2O, and all the others had H_2O:D_2O in the ratio of 90:10. The protein concentrations of uniformly labeled samples were about 5 mM.

NMR spectroscopy

HNCO, HN(CO)CA, HNCA (Grzesiek and Bax, 1992), HN(COCA)HA (Olejniczak et al., 1992), CBCA(CO)NH (Grzesiek and Bax, 1993), HN(CA)HA (Clubb et al., 1992a), HN(CA)CO (Clubb et al., 1992b), HNCACB (Wittekind and Mueller, 1993), COCAH (Dijkstra et al., 1994), HCACO, HCA(CO)N (Powers et al., 1991), HSQC (Bodenhausen and Ruben, 1980), and HOHAHA-HMQC (Marion et al., 1989a) spectra of GlnBP–Gln were recorded. All NMR experiments were carried out at 41 °C.

Most of these experiments were performed on our Bruker AM-500 NMR spectrometer equipped with a 5-mm inverse broadband probe or a 5-mm inverse triple-resonance probe (^1H/^{15}N/^{13}C). The spectrometer was modified by adding homemade and commercial devices to build third and fourth rf channels (parts of the hardware were previously home-built and used to adapt a high-resolution liquid spectrometer to perform solid-state NMR experiments). GARP boxes programmed with different decoupling sequences (Tschudin Associates, Kensington, MD, U.S.A.) were used for X nucleus and proton decoupling. A fast power switch (Tschudin Associates) was

used in some experiments for the X nucleus to switch between pulse and decouple modes. The phases of the third and fourth channels were controlled by a Timing-Simulator (model RS-660, Interface Technology, San Dimas, CA, U.S.A.) in the 'Word Generator' mode, whose output was applied to PTS300 and PTS310 frequency synthesizers (Programmed Test Sources, Littleton, MA, U.S.A.) to create 90°-step phases. The bit pattern was down-loaded to the Timing-Simulator from the ASPECT 3000 under software control via a serial line.

The CBCA(CO)NH experiment was recorded on a Varian Unity 500 spectrometer in Dr. Gordon S. Rule's laboratory at the University of Virginia, Charlottesville, VA, U.S.A. HNCACB was recorded on a Bruker DMX-600 spectrometer by Dr. Clemens Anklin at Bruker Instruments Inc., Billerica, MA, U.S.A.

All 3D triple-resonance experiments except HCACO and HCA(CO)N were performed on a $^{15}N,^{13}C$ uniformly doubly labeled GlnBP sample in H_2O. HCACO and HCA(CO)N were performed on a $^{15}N,^{13}C$ uniformly labeled GlnBP sample in D_2O. HSQC and HOHAHA-HMQC were performed on a ^{15}N uniformly labeled GlnBP sample. HN(COCA)HA was performed as a modified 3D version (no C^{α} frequency labeling) of the 4D experiment. The acquisition parameters for the experiments on the uniformly labeled samples are listed in Table 1.

Water suppression in these experiments was typically achieved by presaturation of the water signal. Quadrature detection in the indirectly detected dimensions was accomplished using the States-TPPI (Marion et al., 1989b) or TPPI (Drobny et al., 1979; Bodenhausen et al., 1980) acquisition methods.

HSQC and 2D versions of the HNCO experiments were also recorded using specifically labeled GlnBP samples in order to obtain specific assignments or amino acid type assignments which were used later as starting points or check markers in the resonance assignment process.

Spectra were processed and peak-picked on a Sun SPARC10 workstation, using the NMRPipe (Delaglio et al., 1995) and PIPP (Garrett et al., 1991) software packages. Linear prediction was used in some cases and zero-filling was used to achieve the final size; data in the F3 dimension ($^1H^N$ or $^1H^{\alpha}$) were usually extracted.

^1H and ^{13}C chemical shifts were referenced to DSS (2,2-dimethyl-2-silapentane-5-sulfonate) at 0 ppm, while ^{15}N chemical shifts were referenced to $(^{15}NH_4)NO_3$ at 24 ppm.

Assignment strategy

A two-step approach has been used to achieve the polypeptide backbone resonance assignment. The first step is to make unambiguous assignments of a number of chosen amino acid residues of GlnBP and use them as starting and check points in later data tracing. This requires the use of specifically labeled GlnBP samples. In addition to the $^1H^N$ and ^{15}N assignments of Trp^{32} and Trp^{220} (Tjandra et al., 1992; Tjandra, 1993), $^1H^N$ and ^{15}N assignments of methionine residues were made. There are three methionines in GlnBP: Met^{48}, Met^{93}, and Met^{144}. Pro^{47}–Met^{48} and Tyr^{143}–Met^{144} are unique pairs in the sequence. The HNCO experiment on the [$^{13}C'$-Pro,^{15}N-Met] sample enabled us to assign $^{13}C'$ of Pro^{47} and $^1H^N$, ^{15}N of Met^{48}. The same experiment was also performed on the [$^{13}C'$-Tyr,^{15}N-U] GlnBP sample. The comparison of the HMQC experiment on [^{15}N-Met] with the above experiments enabled us to assign $^1H^N$-^{15}N of Met^{144}, $^{13}C'$ of Tyr^{143}, and, thus, the $^1H^N$-^{15}N of the remaining Met^{93}.

The experiments on the [$^{13}C'$-Tyr,^{15}N-U] and [$^{13}C'$-Phe, ^{15}N-U] samples in general have not resulted in specific assignments, but they have confined the resulting chemical shifts to a small group of amino acid residues, i.e., tyrosine or phenylalanine and their following residues.

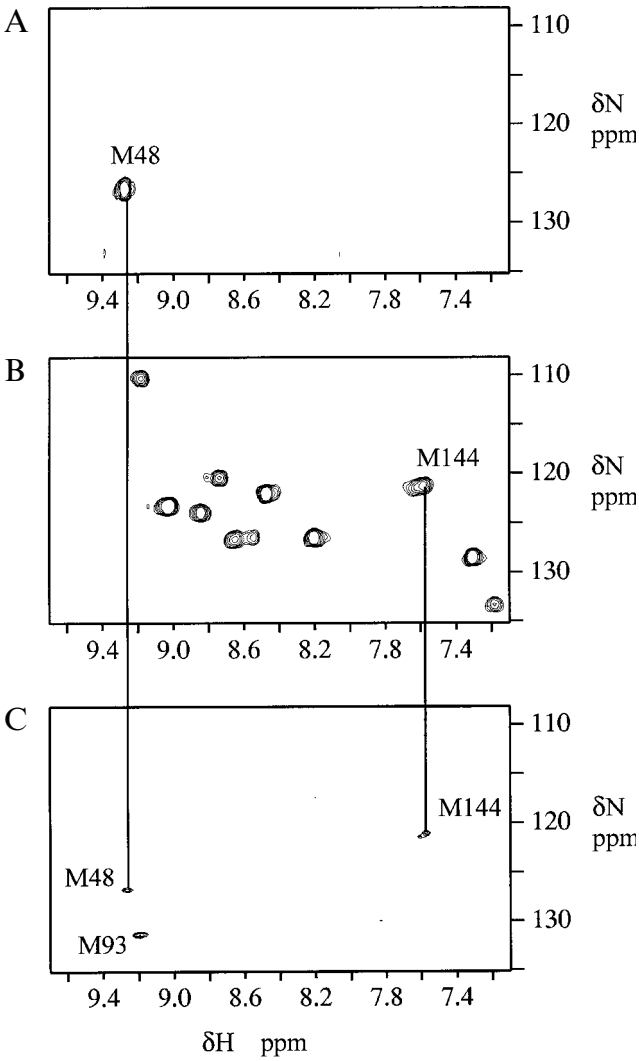

Fig. 3. (A) H-N 2D version of the HNCO experiment on [$^{13}C'$-Pro,^{15}N-Met] GlnBP–Gln in 0.1 M phosphate buffer, 10% D_2O, pH 7.2, at 41 °C. (B) H-N 2D version of the HNCO experiment on [$^{13}C'$-Tyr,^{15}N-other] GlnBP–Gln in 0.1 M phosphate buffer, 10% D_2O, pH 7.2, at 41 °C. (C) HSQC of [^{15}N-Met] GlnBP–Gln in 0.1 M phosphate buffer, 10%D_2O, pH 7.2, at 41 °C.

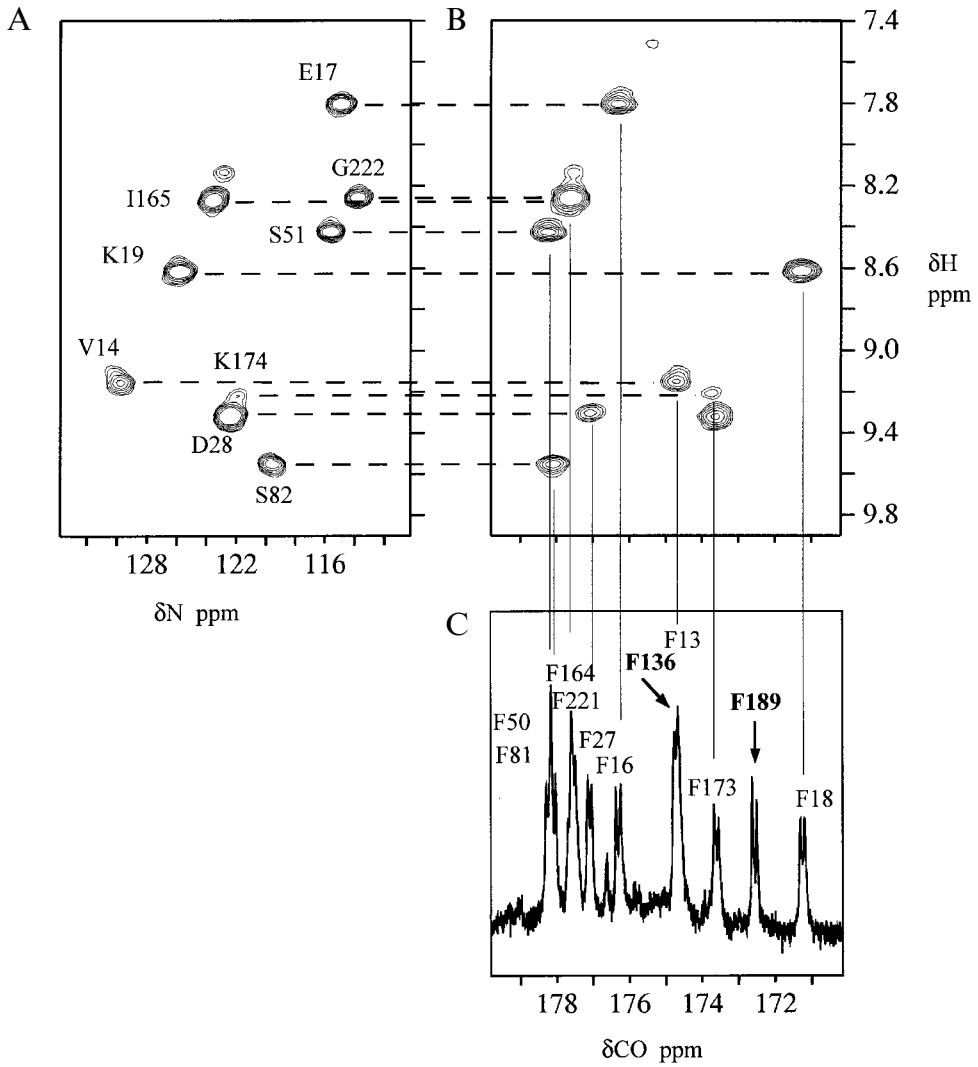

Fig. 4. (A) H-N 2D version of the HNCO experiment on [^{13}C'-Phe,^{15}N-other] GlnBP–Gln in 0.1 M phosphate buffer, 10% D_2O, pH 7.2, at 41 °C. (B) H-C 2D version of the HNCO experiment on the same sample. (C) 1D ^{13}C' spectrum of the same sample. The resonance lines in the spectrum belong to the CO moieties of phenylalanines.

The 1D ^{13}C' spectrum of the [^{13}C'-Pro,^{15}N-Met] sample provided the ^{13}C' chemical shifts of proline residues, one of which has been assigned to Pro[47]. By taking into account the known amino acid sequence information of GlnBP, these chemical shifts provide useful check points for the assignment of the uniformly labeled protein.

The second step is to find sequential connectivities of the backbone resonances. First, we have built chemical shift 'clusters' by comparing and correlating several heteronuclear 3D experiments, so that each cluster is composed of the correlated backbone chemical shifts of one amino acid residue and of its preceding or following residue. We have combined HNCA and HN(CA)CO by matching ^{1}H and ^{15}N chemical shifts to obtain the HNCACO intraresidue chemical shift table. Similarly, we have built up an HNCAHA intraresidue chemical shift table from HNCA and HN(CA)HA data. The interresidue chemical shift table, HNCOCA, can be obtained from HNCO and HN(CO)CA data. We then link these clusters to obtain sequential stretches of chemical shift sets of amino acid residues, starting from one known resonance assignment obtained from experiments on specifically labeled GlnBP samples. For example, starting at the residue i, we look for its amide proton H^N, amide nitrogen N, C^α, and CO chemical shifts in the HNCACO table, and then search for the C^α and CO chemical shifts of its preceding residue $i-1$ in the HNCOCA table. Then, we search for these C^α and CO chemical shifts in the HNCACO table to obtain the H^N and N chemical shifts of residue $i-1$. By alternatively matching pairs of resonances (H^N,N) and (C^α,CO), we proceed to the next amino acid residue, $i-2$, and so on. Similarly, we can also move in the $i+1$ direction. Figure 1 illustrates the procedure that we have used to extend the backbone resonance assignments from a known starting point, Met[93]. Once the amide H^N and N chemical shifts have been determined,

the H^{α} chemical shifts can be obtained from the HNCAHA data.

Because of the large size of the protein (25 kDa), chemical shift degeneracy poses a challenging problem. In the process of either building up one cluster or linking two clusters, we always match two chemical shifts. In case of multiple possibilities, we examine the GlnBP amino acid sequence table and use the amino acid type information provided by the CBCA(CO)NH experiment to make a decision, or we carry out parallel searches for each possible connection until one path leads to the nearest check point. In most cases, a positive decision can be made. If there are too many possibilities, or if the connections are interrupted by missing resonances, we stop and start from another marker.

Results and Discussion

Assignment

Figure 2 shows the 2D ^{1}H-^{15}N-HSQC spectrum of GlnBP–Gln. The resolution is enhanced by linear prediction, shifted sine squared windows, and zero-filling. In the figure, backbone resonances are not labeled, in order to avoid overcrowding. Some side-chain resonances are indicated, such as the $N^{\varepsilon 1}H$ resonances of the tryptophan residues, the NH_2 resonances of asparagine and glutamine residues (linked by horizontal lines), and a resonance folded in from a ^{15}N chemical shift of 86.9 ppm (labeled X). For some of the NH_2 peaks, the isotopically shifted NHD peak is visible upfield in the nitrogen dimension, indicating exchange with the partially deuterated solvent.

The assignment of the three methionine residues is illustrated in Fig. 3. Figure 3A shows the spectrum of the 2D ^{1}H-^{15}N version of the HNCO experiment on the [$^{13}C'$-Pro,^{15}N-Met] GlnBP sample, and provides the $^{1}H^{N}$ and ^{15}N chemical shifts of Met^{48}. Figure 3B shows the result of the same experiment on the [$^{13}C'$-Tyr,^{15}N-U] sample, and provides the $^{1}H^{N}$ and ^{15}N chemical shifts of the residues following tyrosine, one of which is Met^{144}. By comparing this spectrum with the HSQC spectrum of the [^{15}N-Met] sample (Fig. 3C), the resonance peak of Met^{144} is identified. The remaining peak in the HSQC spectrum of the [^{15}N-Met] sample (Fig. 3C) is thus assigned to Met^{93}, since there are only three methionines in GlnBP. All three methionines are now assigned.

The above assignments are unambiguous, but required the preparation of several specifically labeled GlnBP samples. It would be impractical to assign each of the 226

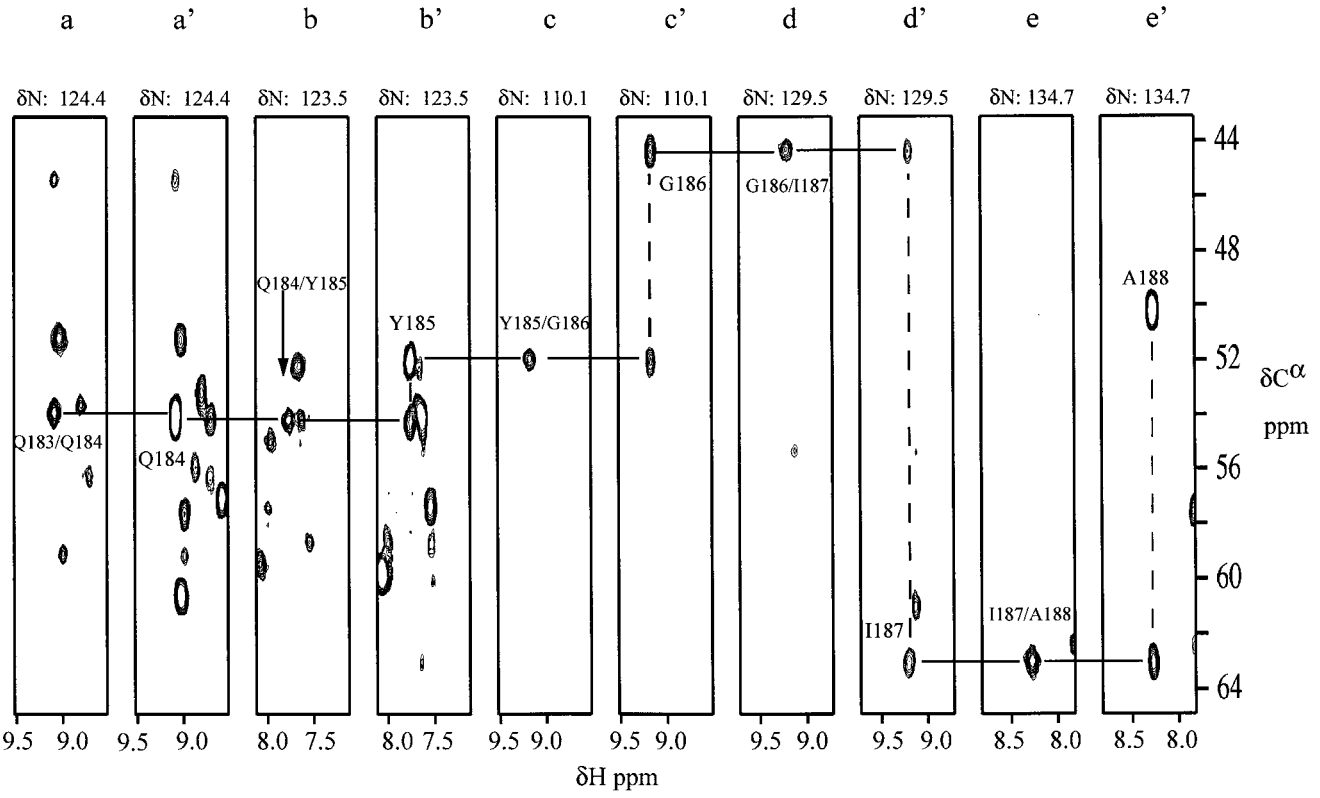

Fig. 5. Strips of the HNCA and HN(CO)CA spectra of ^{13}C,^{15}N uniformly labeled GlnBP, in 0.1 M phosphate buffer, 10% D_2O, pH 7.2, at 41 °C, using a Bruker AM-500 NMR spectrometer. ^{15}N is the third dimension. In the HNCA strips, two resonance peaks are usually obtained for each residue: one is the intraresidue resonance peak, labeled with individual amino acid residue names, and the other is the interresidue resonance peak, labeled with residue pairs. The corresponding HN(CO)CA strips confirm the interresidue resonances. In this figure, the strips containing HNCA and HN(CO)CA resonances of residues 184–188 are shown. a', b', c', d', and e' are HNCA strips; a, b, c, d, and e are their corresponding HN(CO)CA strips.

TABLE 2
BACKBONE AND C^{β} ASSIGNMENT (ppm) FOR GlnBP

Residue	H^N	N	C^{α}	C^{β}	H^{α}	CO	Residue	H^N	N	C^{α}	C^{β}	H^{α}	CO
A1							V62	7.20	113.2	59.5	33.8	4.25	173.3
D2			54.7	41.7	4.62	175.4	D63	8.78	122.3	57.2	44.6	4.60	174.8
K3	8.14	125.3	56.0	33.9	4.31	175.5	L64	7.78	113.9	56.5	41.3	4.39	173.9
K4	8.24	128.4	56.5	33.2	4.18	176.1	A65	8.49	123.4	51.6	25.6	5.05	174.6
L5	8.30	130.9	55.1	43.8	4.42	175.8	L66	7.82	124.3	57.2	44.1	4.79	173.6
V6	10.02	128.7	63.0	32.7	4.32	175.2	A67	8.17	130.6	51.1	19.7	4.97	176.0
V7	8.59	133.9	60.3	32.9	4.06	175.6	G68	8.44	113.5	48.5			172.2
A8	8.54	133.1	51.4	21.1	4.82	175.6	I69	8.75	122.0	62.5	38.5	3.72	175.2
T9	7.53	117.4	59.3	70.8	4.98	171.9	T70	9.58	130.1	64.9	69.3	4.52	174.1
D10	6.89	128.2	54.1	44.7	4.90	175.0	I71	8.43	131.2	62.6	38.3	2.53	175.9
T11	7.63	123.0	66.0	70.6	3.76	177.3	T72	6.39	119.9	58.5	72.4	4.86	174.3
A12	10.29	127.2	54.1	20.3	4.52	174.8	D73			57.9	40.3	4.34	179.2
F13	9.65	134.9	55.6	37.4	5.13	174.8	E74	8.55	123.8	59.8	29.8	4.03	180.7
V14	9.14	129.6	61.2		3.65	173.6	N75	8.06	123.5	60.0	31.7	4.15	178.6
P15			63.5	30.7	3.76	173.0	K76	8.01	123.1	58.9	33.1	5.00	177.5
F16	8.48	130.3	63.5	38.3	3.74	176.4	K77	7.22	120.7	58.7	32.8	4.17	177.0
E17	7.80	114.8	55.1	29.1	5.28	175.2	A78	7.77	124.3	53.4	22.5	4.45	176.4
F18	8.97	122.2	56.7	38.3	4.55	171.3	I79	8.25	117.9	60.2	42.4	4.42	172.5
K19	8.60	125.6	56.3	33.4	3.73	176.1	D80	8.42	121.1	52.5	45.2	5.32	174.9
Q20	8.70	132.9	55.5	32.0	4.48	175.4	F81	8.83	119.4	57.2	45.6	6.11	178.2
G21		121.6[a]					S82	9.53	119.3	59.1	66.7	4.68	173.7
D22			54.3	41.4	4.61	175.3	D83	9.17	123.2	55.6	41.6	4.52	177.2
K23	7.54	122.0	54.9	36.0	4.83	174.2	G84	8.47	112.2	45.9		3.46[b]	175.7
Y24	8.39	125.5	59.1	40.2	4.57	175.7	Y85	8.93	121.0	56.3	41.0	5.26	174.4
V25	8.71	120.3	58.5	36.0	4.57	172.9	Y86	7.29	128.4	60.5	42.1	4.29	172.4
G26	7.35	108.2	43.2		4.06	174.1	K87	7.17	133.1	56.5	32.6	4.22	173.1
F27	7.38	122.8	62.7	39.8	3.39	177.2	S88	8.69	124.6	54.4	68.7	4.60	175.3
D28	9.29	122.5	57.5	39.9	4.48	178.9	G89	9.10	113.9	45.7		3.83, 4.13	171.9
V29	6.27	122.2	66.9	31.8	3.38	178.7	L90	9.08	124.1	54.0	45.8	4.77	174.7
D30	8.58	124.4	57.4	41.9	4.47	179.4	L91	8.79	124.2	53.4	49.0	4.75	174.2
L31	8.66	127.7	58.5	41.7	3.81	178.1	V92	6.82	125.2	62.1	33.2	4.36	173.7
W32	8.66	121.4	59.3	29.2	4.24	176.4	M93	9.20	131.4	54.3	33.2	5.38	174.6
A33	8.25	123.4	55.7	18.3	3.70	180.7	V94	8.82	120.0	59.3	36.7	5.06	176.2
A34	7.63	124.1	55.3	19.0	4.10	180.5	K95	8.97	124.2	57.7	32.4	4.60	178.5
I35	8.06	127.3	66.1	37.7	3.17	176.8	A96	8.22	127.0	55.0		3.60	177.5
A36	8.54	125.2	55.4	18.1	3.25	179.7	N97		116.2[a]				
K37	7.65	121.9	59.3	32.6	4.08	179.7	N98						
E38	7.47	125.0	58.8	29.6	4.03	178.0	N99	10.27[a]	127.1[a]	53.0	40.2	4.99	174.9
L39	7.84	119.0	54.5	42.9	4.20	175.1	D100	8.38	123.2	55.6	42.5	4.66	176.0
K40	7.73	122.6	57.4	29.2	3.86	175.6	V101	7.65	124.7	62.2	32.7	4.14	174.5
L41	8.14	122.3	53.8	44.1	4.68	176.0	K102	9.77	131.3	55.9	33.9	4.42	175.9
D42	8.65	126.8	53.4	43.0	5.03	175.9	S103	8.01	115.9	57.6	66.4	4.44	174.6
Y43	8.18	121.5	56.4	41.4	5.84	172.6	V104	9.69	125.0	64.7	32.0	3.74	176.2
E44	9.01	123.1	54.7	34.0	4.53	174.2	K105	7.74	125.7	57.8	31.9	4.22	178.1
L45	8.72	128.2	54.4	44.3	5.03	177.0	D106	7.57	119.5	55.4	43.2	4.79	175.5
K46	9.02	130.2	52.9	34.8	4.59	171.6	L107	7.53	120.2	55.2	41.4	4.05	176.1
P47		143.6[a]	61.8	32.0	4.33	176.7	D108	6.98	124.6	56.1	39.8	4.13	178.0
M48	9.27	126.7	55.2	36.0	4.43	173.9	G109	9.07	114.6	46.3		3.71, 4.18	174.1
D49	8.18	124.3	54.8	39.7	5.00	179.7	K110	7.82	121.8	54.0	33.7	4.78	176.4
F50	10.03	128.7	62.9	40.1	3.59	178.3	V111	9.89	128.3	62.9	32.6	4.83	176.3
S51	8.40	115.4	61.4	62.4	3.94	174.7	V112	8.26	133.4	60.7	35.1	4.82	173.1
G52	7.92	111.4	45.1		3.66, 4.17[b]	176.0	A113	8.92	134.8	50.3	21.9	5.79	175.3
I53	7.77	128.0	67.1	37.0	3.32	175.9	V114	8.89	115.9	58.4	38.1	4.81	173.9
I54	8.64	123.1	68.5		3.63	176.9	K115	9.19	126.4	54.0	36.0	5.04	175.4
P55		139.4	66.4	31.4	4.28	178.6	S116	9.15	128.6	60.5	64.1	4.16	174.9
A56	7.40	124.0	55.2	18.4	4.01	179.7	G117	9.11	115.2	45.7		3.98, 3.86	174.0
L57	7.96	124.0	57.6	43.3	3.87	179.9	T118	7.30	109.7	60.3	73.3	5.01	177.9
Q58	8.41	121.9	59.5	30.1	4.14	178.6	G119	9.51	113.6	46.7		4.16	175.9
T59	7.70	110.9	61.6	69.6	4.28	173.9	S120	7.69	122.6	61.7	63.7		175.9
K60	7.90	122.0	58.4	28.7	3.84	175.7	V121	7.40	124.3	66.6	31.8	3.36	177.3
N61	8.67	121.3	55.4	40.5	4.56	175.4	D122	6.76	121.7	57.6	40.4	4.16	178.7

TABLE 2
(continued)

Residue	H^N	N	C^α	C^β	H^α	CO	Residue	H^N	N	C^α	C^β	H^α	CO
Y123	8.28	123.8	62.3	38.6	3.86	178.4	A175	8.52	129.2	50.4	21.0	5.34	177.6
A124	8.18	126.4	55.6	19.2	3.81	179.5	V176	8.36	120.2	60.0	35.2	4.51	174.8
K125	8.52	120.0	59.8	32.9	3.94	179.1	G177	8.14	113.1	44.6		3.80, 4.18	172.4
A126	7.36	121.9	54.0	20.0	4.19	179.3	D178	7.72	122.1	52.9	43.2	4.74	175.5
N127	7.52	115.1	55.0	42.1	4.76	174.4	S179	8.19	117.1	58.9	63.2	4.60	175.1
I128	8.48	123.8	60.9	40.3	4.35	176.0	L180	9.86	134.9	53.8	44.8	4.44	177.0
K129	9.00	136.8	54.4	29.5	4.64	177.3	E181	8.45	122.4	55.8	28.3	3.77	174.1
T130	7.65	118.5	61.9	69.2	4.16	175.3	A182	8.01	128.1	54.0	18.4	4.39	178.5
K131	8.88	127.0	58.2	33.3	4.22	176.6	Q183	7.63	121.4	54.3	33.0	4.71	173.1
D132	7.21	118.8	54.4	44.6	4.72	173.1	Q184	9.08	124.4	54.4	33.3	5.09	175.0
L133	8.10	132.1	53.6	42.8	5.18	175.2	Y185	7.76	123.5	52.3	38.2	5.73	175.4
R134	8.96	133.0	55.3	31.8	4.35	173.6	G186	9.15	110.1	44.6		3.54, 4.99	173.4
Q135	8.15	126.0	54.6	30.8	4.91	175.3	I187	9.20	129.5	63.3	38.1	4.19	174.4
F136	8.59	123.8	55.9	43.8[a]	4.88	174.8	A188	8.28	134.7	50.5	24.7	5.01	174.9
P137		138.4	65.3	32.8	4.38	175.9	F189	8.80	119.5	55.4	42.5[b]	4.79	172.7
N138	7.16	112.6	52.0	43.0	5.07	175.6	P190		138.8[a]	62.3	31.9	4.46	178.0
I139	9.14	126.2	59.6	40.1	3.73	175.4	K191	9.07	127.1	57.1	31.86	4.10	178.1
D140	8.52	126.1	57.1	39.7	4.01	178.6	G192	9.07	114.9	45.7		4.25[a]	175.9
N141	7.11	119.1	56.1	39.3	4.19	176.7	S193	8.08	124.4	56.4	62.6	4.86	174.6
A142	6.61	126.0	54.7	17.5	3.26	178.2	D194	7.94	122.5	58.1	40.7	3.74	176.6
Y143	7.70	120.6	58.2	36.4	3.90	179.1	E195	8.30	121.9	60.0	29.6	4.00	178.8
M144	7.58	121.1	58.1	32.3	4.30	178.3	L196	7.89	125.5	57.9	41.8	4.11	177.6
E145	7.44	127.4	58.9	29.5	3.98	178.3	R197	8.00	124.0	59.8	29.6	2.93	177.7
L146	7.53	122.9	57.5	42.6	4.31	179.8	D198	8.33	122.6	57.8	40.3	4.42	180.3
G147	9.01	111.0	47.7		4.38, 3.84	175.4	K199	7.90	125.7	60.0	32.7	4.11	180.1
T148	7.77	113.2	61.9	70.0	4.42	174.7	V200	8.84	127.2	67.6	31.3	3.63	177.3
N149	8.15	119.1	55.1	36.9	4.13[b]	174.8	N201	8.87	124.8	56.1	37.8	4.80	180.1
R150	8.23	122.0	57.9	31.7	4.27	175.5	G202	8.20	112.9	47.6		3.94, 3.99	176.0
A151	7.42	122.5	50.2	21.9	4.39	174.5	A203	8.27	130.2	55.0	19.5	4.32	179.2
D152	9.00	121.6	56.8	44.0	4.60	175.5	L204	8.85	123.7	58.9	42.4	4.15	178.4
A153	7.70	120.1	51.5	25.0	5.25	175.3	K205	7.52	122.6	60.5	32.3	3.96[a]	179.0[a]
V154	9.03	124.5	60.9	36.1	5.11	173.1	T206	8.11	122.6	67.3		3.91	176.2
L155	6.78	131.2	53.3	46.9	5.41	175.1	L207	8.57	123.5	56.9	41.0	4.60	180.9
H156	8.62	126.3	55.8	33.6	5.32	173.2	R208	8.27	124.5	59.7	29.7	4.25	179.1
D157	8.06	122.2	55.1	38.8	5.09	176.6	E209	8.22	123.9	58.8	30.4	4.20	178.4
T158	9.43	127.2	68.2				N210	8.51	119.6	52.5	38.1	4.80	176.9
P159			65.4	31.4	4.44	179.4	G211	7.32	111.1	46.1		3.98, 4.56	175.9
N160	7.11	122.2	57.0	43.2	4.81	175.3	T212	8.82	125.1	67.8		4.02	176.2
I161	7.81	124.9	62.4	36.8	3.77	178.4	Y213	8.29	124.8	63.3	38.7	3.84	176.2
L162	8.33	119.2	58.2	41.7	3.97	180.0	N214	8.45	121.9	56.9	37.8	4.32	177.4
Y163	7.81	124.6	62.4	39.1	3.98	178.8	E215	7.92	124.4	60.0	30.0	4.10	179.6
F164	8.63	126.5	62.4	38.9	3.86	177.7	I216	8.18	126.2	66.1	39.1	3.75	177.7
I165	8.26	123.3	66.6	38.4	3.72	177.6	Y217	8.98	125.8	62.7	39.8	4.36	178.3
K166	7.44	121.2	58.7	33.3	4.03	177.6	K218	8.82	123.9	59.9	32.7	4.15	179.3
T167	7.49	112.8	62.6	70.5	4.11	175.6	K219	7.77	124.9	59.6	32.6	3.67	177.5
A168	8.03	129.9	52.9	20.8	4.27	178.0	W220	7.01	119.4	58.6	31.0	4.30	176.6
G169	7.55	110.3	46.8		3.39[a]	174.6[a]	F221	8.74	119.1	58.7	39.6	4.78	177.7
N170	8.11[a]	124.3[a]	55.6[a]		4.39[a]	176.7[a]	G222	8.26	113.5	46.7		3.94, 4.19	173.2
G171	8.48[a]	112.0[a]		46.1	4.05, 3.69	175.1	T223	7.45	115.5	59.9	70.8	4.63	172.5
Q172	7.94	120.9	56.8	30.2	4.07	176.2	E224	8.24	124.5	55.4[a]	29.5[a]	4.55	174.8[a]
F173	7.76	121.8	56.4	44.1	5.29	173.7	P225		141.1[a]	63.7[b]	31.2[b]	3.85[b]	175.4
K174	9.29	121.9	55.3	36.5	4.77	172.5	K226[b]	7.50	130.9	57.5	34.3	4.10	181.3

[1]H chemical shift is referenced to DSS at 0 ppm; [15]N chemical shift is referenced to $(^{15}NH_4)NO_3$ at 24 ppm; [13]C chemical shift is referenced to DSS at 0 ppm.

[a] Assignments from the automated method.

[b] Tentative assignments.

residues in this way. An alternative method uses amino acid type-labeled GlnBP samples. Figure 4 shows the results of experiments on the [^{13}C'-Phe,^{15}N-U] GlnBP sample. In order to achieve higher resolution, we have conducted the H-N and H-C 2D experiments separately (Figs. 4A and B) instead of running one 3D HNCO. The

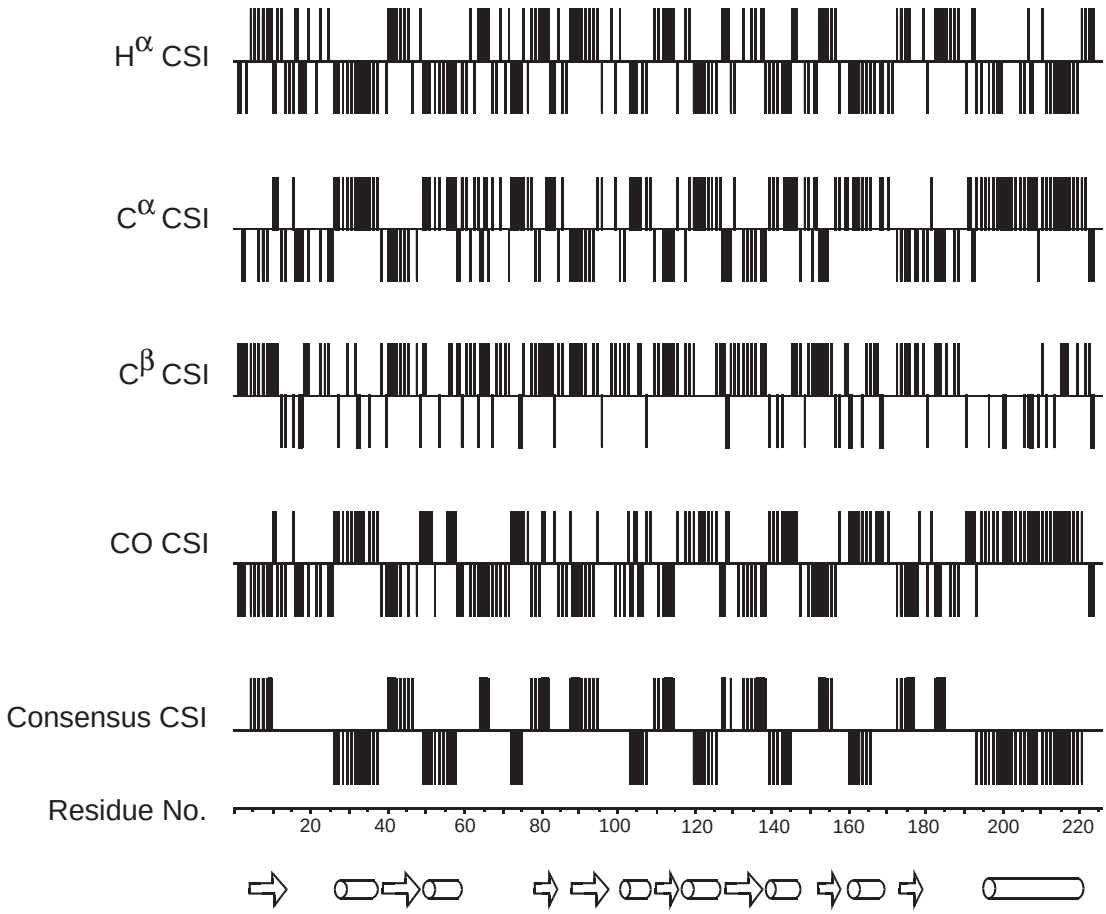

Fig. 6. The chemical shift indices and solution secondary structure for GlnBP–Gln. Arrows represent β-strands and cylinders represent α-helices.

combination of these two experiments has provided the $^{13}C'$ chemical shifts of 9 out of 11 phenylalanines (all except Phe[136] and Phe[189]) and the $^{1}H^{N}$ and ^{15}N chemical shifts of their following residues. There are no HNCO peaks for Phe[136] and Phe[189], since they are followed by proline residues. However, their carbonyl resonances can be found in the 1D $^{13}C'$ spectrum (Fig. 4C). Similar information is obtained by experiments on the [$^{13}C'$-Tyr,^{15}N-U] GlnBP sample.

Of all the 3D triple-resonance experiments, HNCO and HN(CO)CA are the most sensitive. More than 95% of the possible peaks have been observed, providing good information for making the assignments in the i+1 direction.

HNCA is very useful in confirming connections, as it provides both inter- and intraresidue backbone C^{α} chemical shifts. The interresidue C^{α} chemical shifts can be readily identified by comparing the HNCA peaks with resonances in the HN(CO)CA experiment (see Fig. 5).

The HN(CA)CO experiment allowed us to avoid using HCACO and HCA(CO)N data directly in our resonance assignments. Because the latter two experiments have been recorded on a sample in D_2O, the chemical shifts of solvent-exposed residues may differ from those of an H_2O sample. The disadvantage of the HN(CA)CO experiment is its low sensitivity when applied to large proteins like GlnBP. Another drawback is that no HN(CA)CO peaks have been detected for glycine residues. The resulting incompleteness of the HNCACO table made it difficult to link some residues to their preceding neighbors.

Although HN(CA)HA by itself is not a sensitive experiment, by combining its results with those of the HOHAHA-HMQC experiment, most of the (H^{N},N,H^{α}) peaks can be obtained. By comparing and combining these with HNCA, the HNCAHA clusters are built. Together with HN(COCA)HA, this can be a good check for the link to the preceding residue from the HNCACO cluster or a separate pathway when the other link using (C^{α},CO) chemical shifts is not possible.

HCACO and HCA(CO)N have been recorded on a GlnBP–Gln sample in D_2O. Considering that the solvent-induced isotopic effect can affect chemical shifts, we have limited the use of these data in our resonance assignments. These experiments have been used as double or triple checks so that we can get a convincing resonance assignment. They have also helped fill several vacancies when resonance peaks are missing in either HN(CA)HA or HN(CA)CO.

COCAH provides the same information as HCACO and it is almost as sensitive, while avoiding the washout of the H^{α} resonances which are close to water. The very efficient water suppression achieved in our implementation of this experiment has enabled us to run COCAH on the doubly uniformly labeled GlnBP sample in H_2O, providing chemical shifts in excellent agreement with those of the amide H-N detected experiments.

CBCA(CO)NH has been shown to be a very useful experiment with high sensitivity. The correlated (C^{α},C^{β}) chemical shifts provide valuable information about the type of amino acid residues (Grzesiek and Bax, 1993). In particular, most glycine, alanine, serine, and threonine resonances appear in the characteristic regions of the (C^{α},C^{β}) plane. Thus, we are able to use the amino acid sequence information to extend our assignments. The C^{β} assignments made with CBCA(CO)NH have been confirmed by using the less sensitive HNCACB experiment.

The results of backbone and C^{β} resonance assignments are listed in Table 2. A few tentative assignments are indicated; usually they are obtained from one experiment and are not confirmed by another experiment. The assignment for Lys^{226} is also tentative. Because it is the last amino acid residue in the sequence and follows a proline, its chemical shifts cannot be linked with either the preceding or the following residue. We have assigned a strong and narrow resonance peak at 130.9/7.50 ppm in HSQC to H^{N}-N of Lys^{226}, since this residue is at the carbonyl terminus and presumably has high mobility. There is also other supporting evidence. For example, the CO chemical shift corresponding to this H^{N}-N cross peak matches that of Pro^{225}. The CO chemical shift of Pro^{225} is obtained from the 1D ^{13}C spectrum of the [$^{13}C'$-Pro,^{15}N-Met] GlnBP sample, after the other CO resonances are assigned by connections. In addition, the C^{α} and C^{β} chemical shifts of the preceding residue and the assumed Lys^{226} show that this pair could be a Pro-Lys pair.

TABLE 3
COMPARISON OF SECONDARY STRUCTURE FEATURES OF GlnBP OBTAINED FROM THE CSI AND X-RAY DIFFRACTION METHODS

β-Strands			α-Helices		
Designator	Segment		Designator	Segment	
	CSI	X-ray		CSI	X-ray
A	5–10	5–9	I	27–38	27–38
B		11–13	II	50–58	53–58
C		17–20	III		73–78
D		23–25	IV	104–108	
E	41–47	43–47	V	120–126	119–127
F	65–67	64–66	VI	140–145	139–147
G	78–82	79–81	VII	161–166	158–167
H		85–89	VIII	194–209	194–209
I	88–95	90–95	IX	211–221	212–220
J	110–115	111–115			
K	133–139	132–137			
L	153–156	153–157			
M	173–177	172–179			
N	183–185	181–185			
O		186–189			

The crystal structure of unliganded GlnBP is from Hsiao et al. (1996).

Overall, the 3D triple-resonance NMR experiments and specific labeling have enabled us to make a nearly complete backbone resonance assignment (over 95%) of liganded GlnBP. Possible reasons for failing to assign some resonances are discussed at the end of the following section.

A comparison of the manual assignments presented in this paper with the results of the automated assignment method of Lukin et al. (1997) shows that these two sets of resonance assignments agree very well. The assignments of only three H^{N} and about 10 H^{α} are different. More C^{β} assignments are obtained manually than by the automated method, while the automated method provides several assignments which are missing in the manual assignment. These chemical shifts, which we have not confirmed, are indicated explicitly in Table 2.

Secondary structure

The CO, C^{α}, C^{β}, and H^{α} chemical shifts are sensitive to the secondary structure. In fact, the secondary structure can be accurately predicted from these chemical shifts, using the CSI method (Wishart et al., 1992). Figure 6 shows the CSI of CO, C^{α}, C^{β}, and H^{α} for each amino acid residue in GlnBP. The indices have been calculated using the CSI(C) program from the Protein Engineering Network of Centers of Excellence, University of Alberta.

The solution secondary structure of the liganded GlnBP complex obtained by the CSI method is compared with the crystal structure of unliganded GlnBP obtained by X-ray crystallography (Hsiao, 1993; Hsiao et al., 1996). The results are listed in Table 3. Seven α-helices deduced from the CSI agree very well with the X-ray results. The helix predicted for amino acid residues 104–108 is not found in the crystal structure, where amino acid residues 73–78 form an α-helix. Here the CSI fails to show an α-helix positively, but it shows that it is very likely (three adjacent negative bars). All of the 10 β-strands suggested by the CSI match the results from X-ray crystallography, but the X-ray method predicts five more short β-strands, each composed of a couple of amino acid residues.

Overall, the solution secondary structure of the GlnBP–Gln complex determined by the CSI method is very similar to the crystal structure of unliganded GlnBP (Hsiao et al., 1996). Upon ligand binding, the two domains 'close' by stretching or compressing some of the flexible loops or turns, while the α-helices and β-strands remain unchanged.

In the crystal structure of unliganded GlnBP, there are six tight turns located between β-strands: amino acid residues 13–16; 20–23; 49–52; 69–72; 95–98; and 190–193.

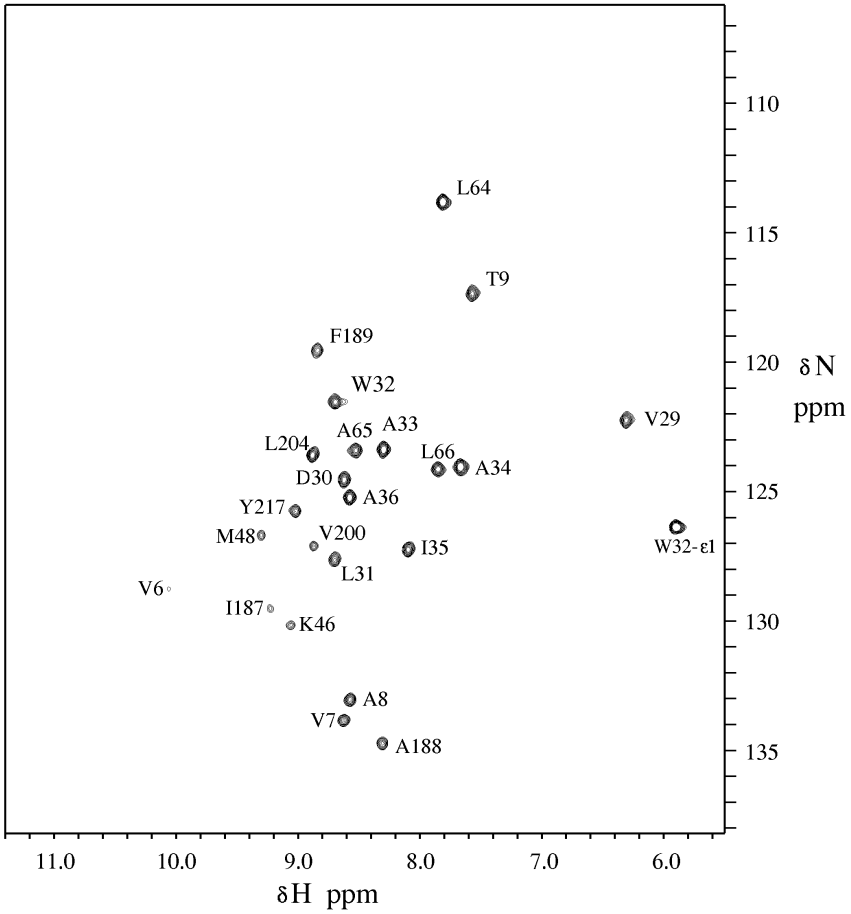

Fig. 7. HSQC spectrum of ^{13}C,^{15}N uniformly labeled GlnBP–Gln in 0.1 M phosphate buffer, >99% D_2O, pH 7.2, at 41 °C, using a Bruker AM-500 NMR spectrometer. The original data size is 512 (F2) × 216 (F1), and the final size is 4096 (F2) × 4096 (F1) with zero-filling in both dimensions and linear prediction in F1. The SW is 3126 Hz in F2 and 8064 Hz in F1. The carrier frequency is at 110 ppm.

Some of them are on the outer surface of the protein molecule. For example, amino acid residues 97–99 occur within a long, exposed loop. This may explain why we have failed to assign some of the backbone NH resonances, such as those of Gly[21], Asp[22], Asp[73], and Asn[97]–Asn[99]. It is possible that the amide protons of these residues exchange rapidly with water and the resonances cannot be observed under our experimental conditions (pH 7.2 and 41 °C).

Solvent accessibility

Figure 7 shows an HSQC spectrum of the [^{13}C'-U,^{15}N-U] GlnBP sample in D_2O. The spectrum contains 24 strong resonance peaks. According to our assignments, these resonances belong to the following amino acid residues: Val[6]–Val[7]–Ala[8]–Thr[9]; Val[29]–Asp[30]–Leu[31]–Trp[32]–Ala[33]–Ala[34]–Ile[35]–Ala[36]; Leu[64]–Ala[65]–Leu[66], Ile[187]–Ala[188]–Phe[189], Lys[46], Met[48], Val[200], Leu[204], and Tyr[217]. The resonance at 126.5/5.88 ppm was unambiguously assigned to the (side-chain) indole $N^{\varepsilon 1}H$ of Trp[32] by using the [indole-^{15}N-Trp]-labeled GlnBP (Tjandra et al., 1992). Since the HSQC experiment (Fig. 7) was carried out at 41 °C and many days after the sample was exchanged into D_2O, the persistence of the amide (^1H,^{15}N) resonances indicates that these amino acid residues are very well protected from exposure to solvent. Among them, there is a stretch of eight amino acid residues, Val[29]–Ala[36], which is part of the α-helix I (residues 27–38) and contains Trp[32]. Both the amide and the side-chain NH of Trp[32] are visible as strong peaks in Fig. 7. This means that this helix fragment and the entire Trp[32] residue are buried inside the protein molecule and are well protected from exposure to the solvent. This finding is totally consistent with, and confirms, our earlier conclusions about the location of Trp[32]. The results of fluorescence (Axelsen et al., 1991) and ^{19}F NMR studies (Shen et al., 1989b) on 6F-Trp-labeled GlnBP have also suggested that Trp[32] is well protected from contact with the solvent. The solvent-induced isotopic shift effect on the ^{19}F resonance is not detected for 6F-Trp[32], while a small effect has been observed for 6F-Trp[220]. While the ^{19}F NMR results could show that one edge of the indole ring is in a hydrophobic region, the data shown in Fig. 7 demonstrate that the entire Trp[32] is in a hydrophobic environment, isolated from the solvent.

As mentioned above, ^{19}F NMR results indicate that

Trp^{220} has some limited, partial exposure to the solvent, at least at one edge of the indole ring. ^1H NMR results have shown that the indole $N^{\varepsilon 1}H$ proton resonance is visible at 11.1 ppm in H_2O, and that this resonance is still visible at room temperature for many hours after the sample was exchanged in D_2O solvent (Shen, 1988; Shen et al., 1989a). This proton resonance was assigned using site-specific mutations (W220F or W220Y), in the spectrum of which the resonance at 11.1 ppm disappeared (Shen et al., 1989b). We do observe this side-chain NH resonance in the HSQC spectrum of GlnBP in H_2O, at 135/11.1 ppm, but not in the HSQC spectrum of the sample in D_2O (this sample was in D_2O for many days and the measurement was at 41 °C). These findings show that Trp^{220} is exchanging slowly with the solvent, while being partially protected. This is consistent with the secondary structure determination, according to which Trp^{220} is located towards the end of the α-helix IX (residues 211–221, see Table 3) which also contains Tyr^{217} (Hsiao et al., 1996). This amino acid residue is well protected from exchange with the solvent, as is proven by the fact that its amide peak can be seen at 125.8/8.98 ppm (Fig. 7).

Our results show that Trp^{32} and Trp^{220} exhibit interesting spectroscopic and structural features. Based on biochemical and molecular biological results, these two tryptophan residues are thought to play an important role in the transport of L-glutamine across the cytoplasmic membrane of *E. coli* (Hunt and Hong, 1983b; Shen et al., 1989b). Further structural and dynamic investigations of GlnBP and the two tryptophan residues will provide new insight into the molecular basis for the ligand-binding and molecular signaling process in this interesting protein.

Conclusions

The recent advances in 3D triple-resonance NMR techniques have enabled us to achieve a nearly complete backbone assignment of GlnBP, a monomeric protein with a molecular weight of 25 kDa. The main difficulty in carrying out the assignment is missing or degenerate resonances and the low sensitivity of some experiments. Specific labeling has been shown to be a useful technique for removing ambiguities and providing starting and check points in resonance assignment. We believe that a combination of modern 3D triple-resonance NMR experiments and specific isotopic labeling will make the assignment of even larger proteins more efficient.

Acknowledgements

We would like to thank Dr. Gordon S. Rule (formerly at the University of Virginia, now at Carnegie Mellon University) for allowing us to perform the CBCA(CO)NH experiment on the Varian Unity 500 NMR spectrometer in his laboratory, and Dr. Clemens Anklin (Bruker Instruments Inc.) for carrying out the HNCACB experiment at Bruker. We thank Dr. Frank Delaglio (NIH) for the NMRPipe software and Dr. Daniel S. Garrett (NIH) for the PIPP software, which we have used to process our NMR data, and Dr. Brian D. Sykes for providing the CSI(C) program. We also thank Mr. Donald G. Bennett for technical support. This work is supported by research grants from NSF (DMB-8816384) and NIH (HL-24525 and GM-26874).

References

Ames, G.F.-L. (1986) *Annu. Rev. Biochem.*, **55**, 397–425.

Ames, G.F.-L. and Joshi, A. (1990) *J. Bacteriol.*, **172**, 4133–4137.

Axelsen, P.H., Bajzer, Z., Prendergast, F.G., Cottam, P.F. and Ho, C. (1991) *Biophys. J.*, **60**, 650–659.

Bodenhausen, G. and Ruben, D.G. (1980) *Chem. Phys. Lett.*, **69**, 185–189.

Bodenhausen, G., Vold, R.L. and Vold, R.R. (1980) *J. Magn. Reson.*, **37**, 93–106.

Clubb, R.T., Thanabal, V. and Wagner, G. (1992a) *J. Biomol. NMR*, **2**, 203–210.

Clubb, R.T., Thanabal, V. and Wagner, G. (1992b) *J. Magn. Reson.*, **97**, 213–217.

Delaglio, F., Grzesiek, S., Vuister, G.W., Zhu, G., Pfeifer, J. and Bax, A. (1995) *J. Biomol. NMR*, **6**, 277–293.

Dijkstra, K., Kroon, G.J.A., Van Nuland, N.A. and Scheek, R.M. (1994) *J. Magn. Reson.*, **A107**, 102–105.

Drapeau, G.R., Brammar, W.F. and Yanofsky, C. (1968) *J. Mol. Biol.*, **35**, 354–364.

Drobny, G., Pines, A., Sinton, S., Weitekamp, D. and Wemmer, D. (1979) *Faraday Symp. Chem. Soc.*, **13**, 49–55.

Furlong, C.E. (1987) In *Escherichia coli and Salmonella: Cellular and Molecular Biology* (Ed., Neidhardt, F.C.), American Society of Microbiology, Washington, DC, U.S.A., pp. 768–796.

Garrett, D.S., Powers, R., Gronenborn, A.M. and Clore, G.M. (1991) *J. Magn. Reson.*, **95**, 214–220.

Grzesiek, S. and Bax, A. (1992) *J. Magn. Reson.*, **96**, 432–440.

Grzesiek, S. and Bax, A. (1993) *J. Biomol. NMR*, **3**, 185–204.

Higgins, C.F., Gallagher, M.P., Hyde, S.C., Mimmack, M.L. and Pearce, S.R. (1990) *Phil. Trans. R. Soc. London*, **B326**, 353–365.

Hsiao, C.-D. (1993) Ph.D. Thesis, University of Pittsburgh, Pittsburgh, PA, U.S.A.

Hsiao, C.-D., Sun, Y.-J., Rose, J. and Wang, B.-C. (1996) *J. Mol. Biol.*, **262**, 225–242.

Hunt, A.G. and Hong, J.-S. (1981) *J. Biol. Chem.*, **256**, 11988–11991.

Hunt, A.G. and Hong, J.-S. (1983a) *Biochemistry*, **22**, 844–850.

Hunt, A.G. and Hong, J.-S. (1983b) *Biochemistry*, **22**, 851–854.

Hyde, S.C., Emsley, P., Hartshorn, M.J., Mimmack, M.M., Gileadi, U., Pearce, S.R., Gallagher, M.P., Gill, D.R., Hubbard, R.E. and Higgins, C.F. (1990) *Nature*, **346**, 362–365.

Kang, C.H., Shin, W.-C., Yamagata, Y., Gokcen, S., Ames, G.F.-L. and Kim, S.-H. (1991) *J. Biol. Chem.*, **266**, 23893–23899.

Lukin, J.A., Gove, A.P., Talukdar, S.N. and Ho, C. (1997) *J. Biomol. NMR*, **9**, 151–166.

Mao, B., Pear, M.R., McCammon, J.A. and Quiocho, F.A. (1982) *J. Biol. Chem.*, **257**, 1131–1133.

Marion, D., Driscoll, P.C., Kay, L.E., Wingfield, P.T., Bax, A., Gronenborn, A.M. and Clore, G.M. (1989a) *Biochemistry*, **28**, 6150–6156.

Marion, D., Ikura, M., Tschudin, M.R. and Bax, A. (1989b) *J. Magn. Reson.*, **85**, 393–399.

Newcomer, M.E., Gilliland, G.L. and Quiocho, F.A. (1981) *J. Biol. Chem.*, **256**, 13213–13217.

Olejniczak, E.T., Xu, R.X., Petros, A.M. and Fesik, S. (1992) *J. Magn. Reson.*, **100**, 444–450.

Powers, R., Gronenborn, A.M., Clore, G.M. and Bax, A. (1991) *J. Magn. Reson.*, **94**, 209–213.

Quiocho, F.A., Vyas, N.K., Sack, J.S. and Storey, M.A. (1987) In *Crystallography in Molecular Biology* (Eds, Moras, D., Drenth, J., Strandberg, B., Such, D. and Wilson, K.), Plenum, New York, NY, U.S.A., pp. 385–394.

Quiocho, F.A. (1990) *Phil. Trans. R. Soc. London*, **B326**, 341–352.

Sharff, A.J., Rodseth, L.E., Spurlino, J.C. and Quiocho, F.A. (1992) *Biochemistry*, **31**, 10657–10663.

Shen, Q. (1988) Ph.D. Thesis, Carnegie Mellon University, Pittsburgh, PA, U.S.A.

Shen, Q., Simplaceanu, V., Cottam, P.F. and Ho, C. (1989a) *J. Mol. Biol.*, **210**, 849–857.

Shen, Q., Simplaceanu, V., Cottam, P.F., Wu, J.-L., Hong, J.-S. and Ho, C. (1989b) *J. Mol. Biol.*, **210**, 859–867.

Spurlino, J.C., Lu, G.-Y. and Quiocho, F.A. (1991) *J. Biol. Chem.*, **266**, 5202–5219.

Tjandra, N., Simplaceanu, V., Cottam, P.F. and Ho, C. (1992) *J. Biomol. NMR*, **2**, 149–160.

Tjandra, N. (1993) Ph.D. Thesis, Carnegie Mellon University, Pittsburgh, PA, U.S.A.

Vyas, N.K., Vyas, M.N. and Quiocho, F.A. (1991) *J. Biol. Chem.*, **266**, 5226–5237.

Weiner, J.H. and Heppel, L.A. (1971) *J. Biol. Chem.*, **246**, 6933–6941.

Wishart, D.S., Richards, F.M. and Sykes, B.D. (1992) *Biochemistry*, **31**, 1647–1651.

Wittekind, M. and Mueller, L. (1993) *J. Magn. Reson.*, **B101**, 201–205.

Wüthrich, K. (1986) *NMR of Proteins and Nucleic Acids*, Wiley, New York, NY, U.S.A.